Structural Characterization of a Serendipitously Discovered Bioactive Macromolecule, Lignin Sulfate

Arjun Raghuraman,[†] Vaibhav Tiwari,[||] Jay N. Thakkar,[†,§] Gunnar T. Gunnarsson,[†,§] Deepak Shukla,[||] Michael Hindle,[‡] and Umesh R. Desai*[,†,§]

Departments of Medicinal Chemistry and Pharmaceutics, and Institute for Structural Biology and Drug Discovery, Virginia Commonwealth University, Richmond, Virginia 23298-0540, and Departments of Opthalmology, Visual Sciences, Microbiology, and Immunology, University of Illinois at Chicago, Chicago, Illinois 60612

Received May 4, 2005; Revised Manuscript Received June 10, 2005

The herpes simplex virus-1 (HSV-1) utilizes cell-surface glycosaminoglycan, heparan sulfate, to gain entry into cells and cause infection. In a search for synthetic mimics of heparan sulfate to prevent HSV infection, we discovered potent inhibitory activity arising from sulfation of a monomeric flavonoid. Yet, detailed screening indicated that the sulfated flavonoid was completely inactive and the potent inhibitory activity arose from a macromolecular substance present in the parent flavonoid. The active principle was identified through a battery of biophysical and chemical analyses as a sulfated form of lignin, a three-dimensional network polymer composed of substituted phenylpropanoid monomers. Mass spectral analysis of the parent lignin and its sulfated derivative indicates the presence of *p*-coumaryl monomers interconnected through uncondensed β-*O*-4-linkages. Elemental analysis of lignin sulfate correlates primarily with a polymer of *p*-coumaryl alcohol containing one sulfate group. High-performance size exclusion chromatography shows a wide molecular weight distribution from 1.5 to 40 kDa suggesting significant polydispersity. Polyacrylamide gel electrophoresis (PAGE) analysis indicates a highly networked polymer that differs significantly from linear charged polymers with respect to its electrophoretic mobility. Overall, macromolecular lignin sulfate presents a multitude of substructures that can interact with biomolecules, including viral glycoproteins, using hydrophobic, hydrogen-bonding, and anionic forces. Thus, lignin sulfate represents a large number of interesting structures with potential medicinal benefits.

Introduction

Herpes simplex viruses (HSV) are human enveloped viruses that cause mucocutaneous lesions of the mouth, face, eyes, or genitalia.[1,2] These infections are highly prevalent, affecting at least 1 in 3 individuals in the U.S. Occasionally, the virus spreads to the central nervous system causing meningitis or encephalitis. Of the eight herpes viruses known to infect humans, HSV-1 is the most common, causing cold sores in the mouth, and is readily transmitted through routine intimate contact.[3] HSV infection of cells involves several molecules, especially glycoproteins gB, gC, and gD (viral glycoprotein D), which are known to be present on the viral envelope.[3−6] These viral glycoproteins interact with heparan sulfate (HS) chains present on cell surface to enhance the efficiency of infection. Removal of HS chains from the cell surface through enzymatic treatment or presence of soluble forms of HS severely retards HSV entry into cells.

Heparan sulfate, a glycosaminoglycan covalently attached to the protein core of proteoglycans, is widely expressed in human tissues and has important roles in development, differentiation, and homeostasis.[7,8] Structurally, HS is a linear copolymer of glucosamine (GlcNp) and glucuronic acid (GlcAp) residues linked in a 1→4 manner, of which the GlcNp residue are typically acetylated at 2-position.[9,10] Despite this apparently simple monomeric disaccharide structure, heparan sulfate perhaps represents the most complex molecule nature biosynthesizes because of additional apparently indiscriminate epimerization of some GlcAp residues to iduronic acid (IdoAp) and sulfation of only some available −OH groups. This primary structural diversity is further complicated by another level of complexity wherein sulfate groups may cluster in small regions and form differentially charged mini-domains. A simple calculation of a number of structural sequences possible with these variations, especially of the size recognized by proteins and receptors, shows millions of possibilities. The structural richness of HS is arguably the origin for its involvement in numerous biological processes. Yet, specific recognition sequences may be critical. A good example of specific recognition is demonstrated by the HS−gD interaction, wherein a 3-*O*-sulfated GlcNp residue is essential for HSV-1 to penetrate cells.[11,12]

* To whom correspondence should be addressed. Phone: (804) 828-7328. Fax: (804) 827-3664. E-mail: urdesai@vcu.edu.

[†] Department of Medicinal Chemistry, Virginia Commonwealth University.

[‡] Department of Pharmaceutics, Virginia Commonwealth University.

[§] Institute for Structural Biology and Drug Discovery, Virginia Commonwealth University.

[||] University of Illinois at Chicago.

10.1021/bm0503064 CCC: $30.25
Published on Web 00/00/0000

A simple approach to inhibiting HSV entry into cells would be to competitively bind the virus with HS-like molecules. In this regard, numerous sulfated molecules have been explored including heparin and its chemically modified derivatives,[13−15] pentosan polysulfate,[16] dextran sulfate,[16,17] sulfated maltoheptaose,[16] sulfated fucoidans,[18−20] spirulan,[21] sulfated galactans,[22,23] and miscellaneous sulfated polysaccharides.[24−27] Not unexpectedly, HS mimics found to-date to inhibit viral entry have a linear polysaccharide backbone with varying degrees of sulfation. We reasoned that it should be possible to efficiently inhibit HSV entry into cells using nonpolysaccharide sulfated compounds, especially in light of a 1964 report by Vaheri et al.[28] Toward this end, we screened a library of sulfated flavonoids, which we had synthesized earlier,[29−32] to discover a high activity molecule that had no resemblance to the structures present in our library. This paper describes the structural characterization of a serendipitously discovered macromolecule that inhibits HSV-1 entry into cells. The bioactive macromolecule is a sulfated derivative of lignin, a polymer made up of repeating phenylpropanoid units. Structurally, lignin sulfate presents a rich array of hydrophobic, hydrogen-bonding, and anionic domains possessing strong potential for interacting with biomolecules, including viral glycoproteins, and possibly mimicking heparan sulfate.

Experimental Section

Chemicals. Morin was obtained from Indofine (Somerville, NJ), Fluka (Milwaukee, WI), and Aldrich (Milwaukee, WI). Polystyrene sulfonate standards (PSS) of nominal molecular weights 145, 80, 30, 15, 7, and 2 kDa were from American Polymer (Mentor, OH). *N*,*N*-Dimethyl-*m*-phenylenediamine dihydrochloride, *N*,*N*-dimethyl-*p*-phenylenediamine monohydrochloride, sulfur trioxide-triethylamine complex, and NP-40 were from Sigma-Aldrich (Milwaukee, WI). β-Galactosidase substrate and *o*-nitrophenyl β-D-galactopyranoside (ONPG) were from Pierce (Rockford, IL). High purity water, obtained from NERL Diagnostics (RI), was used in all experiments. Elemental analysis of lignin sulfate fractions was obtained from Atlantic Microlabs (Norcross, GA).

Cells and Viruses. Dr. Patricia Spear (Northwestern university) provided HeLa cells and the reporter viruses listed here. HSV-1 virus strain carrying the *lacZ* gene of *E. coli* and capable of expressing β-galactosidase as a reporter of entry included HSV-1(KOS) gL86,[33] and HSV-1(KOS)-tk12.[34] The experiments shown here were done with HSV-1(KOS)gL86 alone.

HSV-1 Virus Infection Assay. Assays for infection of cells were based on quantitation of β-galactosidase expressed by the mutant HSV-1 viral genome containing the *lacZ* gene.[11,12] HeLa cells were grown in 96-well tissue culture dishes ($(2-4) \times 10^4$ cells/well), washed after 16 h of growth, and exposed to 10 plaque forming units (PFU)/cell of HSV-1 virus in 50 μL of phosphate-buffered saline (PBS) containing glucose and 1% calf serum (PBS-G-CS) for 6 h at 37 °C. To test for inhibitory activity, the sulfated compounds were simultaneously added to this 50 μL medium in varying amounts ranging from 0.2 μg to 1.6 ng. Following incubation, the cells were solubilized in 100 μL of PBS containing 0.5% NP-40 and 10 mM ONPG. The initial rate of hydrolysis of the substrate was monitored spectrophotometrically (Spectra MAX 190, Molecular Devices) at 410 nm, which corresponds to the concentration of the β-galactosidase within HeLa K-1 cell. The initial rate of hydrolysis of the substrate in the absence of any added sulfated molecule formed the control and assigned a value of 100% HSV-1 infection. Assays were performed in duplicate and analyzed using equation 1 to obtain IC_{50} values. For comparison of IC_{50} values for the sulfated polymer obtained by two methods, purified either from sulfation reaction of natural product morin or from sulfation of purified polymer from morin, weight-based concentrations were used, after ascertaining that the electrophoretic profiles are similar.

$$F = F_{MIN} + \frac{F_{MAX} - F_{MIN}}{1 + 10^{(\log[I]_O - \log IC_{50}) \times b}} \quad (1)$$

where F is the absorbance at 410 nm at inhibitor concentration $[I]_O$, F_{MAX} and F_{MIN} are the maximal and minimal values of this absorbance, IC_{50} is the concentration of inhibitor that gives 50% inhibition, and b is the Hill slope of the curve.

Gel Electrophoresis. PSS, morin persulfate (MoS), and higher molecular weight fractions of lignin sulfate were analyzed using a protocol commonly for proteins. The electrophoresis run buffer was 100 mM Tris, and 100 mM boric acid buffer, pH 8.3, containing 2 mM EDTA. PSS and lignin sulfate samples were analyzed using gel concentrations ranging from 6% to 18%. No stacking gel was used. The samples, 10 μg in 4 μL of standards and 30 μg in 4 μL of polymer fractions, were loaded onto the resolving gel using 40% glycerol. Electrophoresis was performed at a constant current. The gels were stained for 10 min using the high-iron diamine stain[35] followed by destaining with water for 24 h. Densitometric analysis was performed using BioRad VersaDoc 4000 ChemImager equipped with a 610 nm filter against a transwhite background. Relative front (R_f) of bands, defined as the ratio of band migration distance to the length of gel, were calculated using BioRad Quantity 1 software. The mobility of a band was then calculated by multiplying its R_f value by gel length and factoring in the run time.

Capillary Electrophoresis. Capillary electrophoresis of morin sulfate and unknown sulfated polymer was carried out under reverse polarity conditions using a Beckmann PACE/MDQ unit. An uncoated fused silica capillary of 50 μm internal diameter and 32.5 cm effective length to the detector window was used. Samples were typically injected under a pressure of 0.5 psi for 10 s and detected spectrophotometrically using a 254 nm filter. Electrophoresis was performed at 25 °C and a constant voltage of 5 kV using 100 mM sodium phosphate, pH 2.7.

Nuclear Magnetic Resonance (NMR) Spectroscopy. Low molecular weight sulfated polymer sample for NMR analysis was prepared as follows. The filtrate from the 5 kDa molecular weight filter was lyophilized, and the solid was loaded on a Sephadex G-25 column. Elution with water separated the polymer (M_R = 1.9 kDa) from the monomer,

morin sulfate. The polymer sample was lyophilized twice from ^2H_2O, and ^1H NMR spectra were recorded on a 500 MHz Oxford-Varian spectrometer in ^2H_2O at either 25, 30, 40, or 50 °C. ^{13}C NMR spectrum was recorded on a 300 MHz Varian-Gemini spectrometer at 60 °C. For ^{13}C NMR analysis, nearly 60 mg of the polymer was dissolved in 0.75 mL of ^2H_2O and the signal acquired for 20 272 scans with an acquisition time of 1.7 s and a pulse delay of 2 s. A line-broadening factor of 50 Hz was used to extract the ^{13}C NMR spectrum of the polymer from noise.

Reverse-Phase HPLC. The analysis of morin, ethyl acetate, or acetone insoluble substance (polymeric contaminant of morin), phloroglucinol adducts, or acid butanol products was performed on a Shimadzu VP system. Typically samples (0.1 mg/mL) were analyzed using a YMC ODS-AQ S-5 120A (Waters, Milford, MA) 4.6 × 250 mm column in analytical mode. A guard column was used to remove any particulate matter. The mobile phase consisted of an acetonitrile−water mixture (either 1:1 or 7:3 v/v) at a constant flow rate of 0.1−0.5 mL/min. Detection was performed at 279 nm.

Isolation of Polymeric Product from the Natural Product, Morin. Morin (5 g) was stirred in 400 mL of ethyl acetate at room temperature for 2 h, following which the precipitate so remaining was filtered on Whatman filter paper (No. 1). The precipitate so obtained was dissolved in 70% ethanol−water mixture, and the solution was filtered through Amicon centrifugal concentrator with membrane filter 5K. The retentate on the membrane was evaporated to give the parent polymer in ∼10% yield.

Sulfation of Polymeric Substance. The parent polymeric sample (0.5 g) was sulfated using TEAST complex (3.2 g) at 65 °C in *N*,*N*-dimethyl acetamide (DMA) for 3 h in the presence of molecular sieves.[29−31] Following the reaction, the mixture was poured in acetone containing 0.5−2 mL of triethylamine, and the solution was left undisturbed at 4 °C for 24 h. A crude oil formed at the bottom. This oil was collected, washed with chilled acetone, and suspended in 30% sodium acetate. After about 2 h, the suspension was added to 50 mL of ethanol to precipitate the sodium salt of the sulfated polymer (0.2 g).

Acid-Butanol Test for Condensed Tannins. The acid-butanol test for condensed tannins essentially followed previous protocol.[36] Briefly, two reagents were prepared. Reagent A consisted of a butanol−HCl mixture (95:5 v/v), while reagent B consisted of 2% ferric ammonium sulfate in 2 N HCl. A small amount of the polymeric sample (1−5 mg) was dissolved in 0.5 mL of aqueous acetone (70%) so that the absorbance at 550 nm is less than 0.6. To this solution was added 3.0 mL of reagent A and 0.1 mL of reagent B. The tube was vigorously shaken on a vortexer, tightly covered, and heated at 100 °C for 1 h, after which its A_{550} value was recorded.

Phloroglucinol Test for Condensed Tannins. The phloroglucinol test for condensed tannins followed the previously developed protocol.[37] Briefly, a solution of 0.1 N HCl in methanol containing 50 g/L phloroglucinol and 10 g/L ascorbic acid was prepared. To this solution (20 mL) was added the ethyl acetate or acetone insoluble substance (100 mg), and it was heated at 50 °C for 20 min. The final solution was brought to room temperature, combined with 100 mL of 40 mM aqueous sodium acetate, and analyzed by reverse-phase high performance liquid chromatography (RP-HPLC).

Mass Spectrometric Identification of Lignin Oligomers. A solution of 200 mg of lignin in 10 mL of 0.2 M HCl in dioxane−methanol (1:1 v/v) was refluxed for 24 h, cooled, and treated with 0.2 M aqueous NaOH to neutralize the acid. The reaction mixture was worked up in a standard manner using ethyl acetate to get a mixture of lignin products, which were analyzed using LC−MS. The LC−MS system consisted of a Waters Alliance 2690 separation module and a Waters 996 photodiode array (PDA) UV detector (Waters Corp., Milford, MA). Chromatographic separation was achieved using an analytical Discovery C18 column (Supelco, Bellefonte, PA, 4.6 × 150 mm) and a linear binary gradient consisting of water−methanol (50:50 v/v) (solvent A) and methanol (solvent B) at a flow rate of 1 mL/min over period of 30 min. Eluent peaks were monitored at 279 nm and then analyzed by mass spectrometry. Liquid eluent was delivered to a Micromass ZMD4000 single quadrupole mass spectrometer with ACPI ionization probe operating in negative ion mode (Waters Corp., Milford, MA). Optimized MS ionization conditions were employed; the source block temperature and the APCI probe temperature were held at 100 and 40 °C, respectively. Corona and cone voltages of 3.5 kV and 52 V were selected following optimization. The desolvation nitrogen flow was 400 L/h. Mass spectra were acquired in the mass range from 100 to 1100 Da at 400 amu/s.

Fractionation of Lignin Sulfate Mixture Using Centrifugal Filtration. The dark brown reaction mixture (1.2 g) from sulfation of polymeric lignin was dissolved in water (6 mL) and filtered through a Millipore filter (nominal molecular weight cutoff (NMWC) 100 kDa) at 4000 g. Filtration was performed until the final volume of the retentate was 100 μL. Water (4 mL) was added to the retentate, and the process was repeated with successive portions of water until the filtrate appeared colorless. The retentate was labeled as 100 kDa fraction. The combined filtrate from the 100 kDa filter was then filtered through a 50 kDa filter to obtain a 50 kDa fraction. This process was further repeated for 10 and 5 kDa filters to obtain 10 and 5 kDa fractions. The retentates, 100−5 kDa, were collected and lyophilized to obtain four fractions in yields of 3.2%, 0.9%, 2.7%, and 1.7%, respectively. The filtrate from the 5 kDa filter was lyophilized to obtain a mixture of morin sulfate and low molecular weight polymer.

Determination of Molecular Weight of Lignin Sulfate Fractions Using HP-SEC. The HP-SEC analysis was carried out on a Shimadzu chromatography system composed of LC10Ai pumps and a SPD-10A VP UV-vis detector controlled by a SCL-10A VP system controller connected to a computer. Fractions of 100, 50, 10, and 5 kDa were analyzed using ASAHIPAK GS 520 HQ (Phenomenex, Torrance, CA, 7.6 mm i.d. × 300 mm). A guard column (Phenomenex) was used to remove particulates, if present. The mobile phase consisted of a 100 mM sodium chloride−acetonitrile mixture (7:3 v/v) at a constant flow rate of 0.4 mL/min. PSS samples

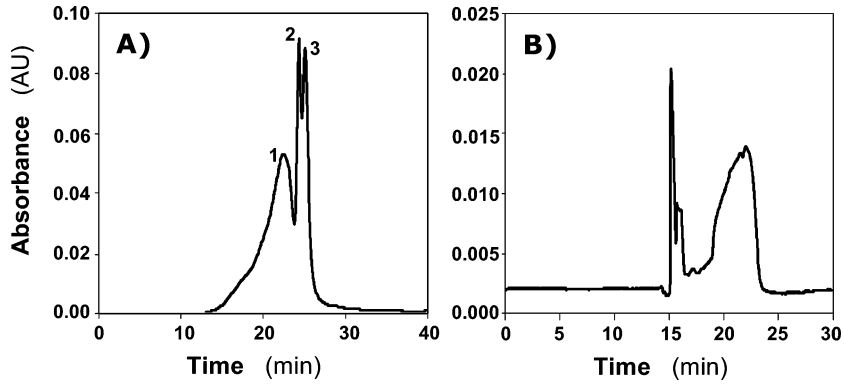

Figure 1. High performance size exclusion chromatographic (A) and capillary electrophoretic (B) analysis of sulfation reaction of morin. HP-SEC was performed on an analytical column using acetonitrile−water (7:3 v/v) mobile phase at 0.4 mL/min, while CE was performed using an uncoated silica capillary in reverse polarity mode with 100 mM sodium phosphate buffer, pH 2.7, at 5 kV. Peaks were detected at 266 and 254 nm in HP-SEC and CE, respectively. Broad unsymmetrical peaks between 14 and 24 min (peak 1) in HP-SEC (A) and 19−23 min in CE (B) correspond to the sulfated polymeric substance present in morin sulfate reaction mixture. Peaks 2 and 3 in (A) are monomeric morin sulfate reaction products. See text for details.

of 145, 80, 30, 15, 7, and 2 kDa and morin persulfate (M_W = 835) were used as standards. Detection was performed at 226 nm for standards and at 266 nm for morin persulfate and higher molecular weight fractions.

Average molecular weights (M_R) were determined by HP-SEC using ASAHIPAK GS 520 HQ column and 100 mM sodium chloride−acetonitrile (7:3 v/v) as mobile phase. A standard calibration curve was prepared using polystyrene sulfonate samples of defined M_R 145, 80, 30, 15, 7, and 2 kDa, and morin per-sulfate (M_W = 835). A semilogarithmic linear dependence between M_R and retention time (RT) was obtained (log M_R = 8.3 − (0.2 × RT)) with a correlation coefficient of 0.99. This equation was tested on full-length heparin and low molecular weight heparin samples of known M_R (14.9 and 5 kDa). Heparin and low molecular weight heparin eluted at 19.0 and 21.8 min, corresponding to M_R of 16 and 4 kDa, respectively, suggesting good predictability.

Results

Crude Morin Sulfate Reaction Mixture Inhibits HSV-1 Infection. In a screen for determining the ability of sulfated flavanoids and flavonoids as inhibitors of HSV-1 infection, we utilized a standard viral infection assay used earlier.[11,12] Briefly, in this assay, a mutant strain of HSV-1 that contains the *lacZ* gene is used so as to enable a spectrophotometric determination of infection. The method is simpler and less tedious than a plaque formation assay used earlier. This HSV-1 viral infection inhibition assay involves the exposure of a constant dose of virus to HeLa cells, which internalize the virus, in the presence and absence of sulfated inhibitors. Following incubation for 6 h at 37 °C, the internalized viral particles are quantified using the β-galactosidase activity of the viral genome, which decreases in a sigmoidal manner (eq 1) as the concentration of the sulfated inhibitor increases.

Several sulfated flavanoids and flavonoids were screened including (+)-catechin sulfate, (−)-epicatechin sulfate, quercetin sulfate (QS), and morin sulfate (MoS), each containing multiple sulfate groups. These sulfated flavanoids and flavonoids were synthesized as previously reported[29,31,32] from their respective phenolic precursors, which are typically isolated from plants. Except for MoS, none of the sulfated flavonoids displayed any activity at concentrations as high as 1−2 mM. In contrast, entry of HSV-1 into HeLa cells decreased steadily from ∼100% to ∼15% for morin sulfate as the concentration was increased to 250 μM (not shown). (This phenomenon was also true for HSV type 2 strain and for HIV-1. Details regarding inhibition of HSV (HSV-1 and HSV-2) and HIV-1 entry into cells (IC_{50}, Hill slope, M_R dependence) will be published elsewhere.) This suggested that only MoS inhibited HSV-1 entry into mammalian cells. Paradoxically, however, it suggested an exquisite specificity in this inhibition because MoS differs from QS in the position of only one $-OSO_3^-$ group, yet QS showed absence of inhibitory activity at concentrations as high as 2 mM.

To test whether such exclusive specificity has a structural basis, MoS and QS were resynthesized and rigorously purified. It is important to note at this point that the ^{1}H NMR spectrum of starting natural product morin and crude MoS reaction mixture did not show peaks other than those for morin and morin sulfate, respectively, except for a rolling baseline, thus making it difficult to assess the purity of products. Yet, repeated purification steps followed by bioassay showed near absence of HSV-1 infection inhibition activity in both purified MoS and QS. At the same time, the partially purified MoS reaction mixture continued to display good activity in inhibiting HSV-1 infection. Thus, we reasoned that HSV-1 entry into cells was being inhibited by a substance other than the monomeric MoS, which was absent in other flavonoids.

HSV-1 Infection Inhibition Activity Arises from a Polysulfated Polymer. To better understand the sulfated product, high performance size exclusion chromatography (HP-SEC) and capillary electrophoresis (CE) of the MoS reaction mixture was performed. HP-SEC, using water−acetonitrile (7:3 v/v) mobile phase and an analytical column that resolves molecules up to 40 000 Da, showed two peaks at ∼24 and ∼26 min (peaks 2 and 3), and a broad, unsymmetrical peak between 14 and 24 min (peak 1, Figure 1A). Electrospray ionization mass spectroscopy (ESI-MS) of peak 2 in positive ion mode revealed a molecular ion $[M + 6Na]^+$ at m/z = 834.75 Da corresponding to morin

skeleton functionalized with five sulfate groups (MoS, not shown). Based on its elution pattern, peak 3 is likely to be tetrasulfated morin. In addition, CE of the crude MoS reaction mixture under reverse polarity conditions at 25 °C in 100 mM sodium phosphate buffer, pH 2.7, showed the presence of peaks at ~15 and ~16 min, and a broad peak between 19 and 24 min (Figure 1B). The peak at ~15 min in CE was identified as the monomeric MoS by injecting the purified sulfated flavonoid under similar conditions, while the broad peak did not resolve even with exhaustive changes in capillary voltage, type of buffer, its pH, and the ionic strength of buffer. Such broad peak profiles are typical of heterogeneous, polydisperse anionic polymers exemplified by full-length and low-molecular-weight heparins (LMW-H),[38−40] thus implying the presence of an unexpected polysulfated polymer in the MoS reaction mixture. Further, the detectability of this polymer in HP-SEC and CE, but not in ^{1}H NMR, indicated that the polymer was highly heterogeneous, and possibly polydisperse, with each chain constituting an exceedingly small proportion of the overall content.

To assess whether HSV-1 infection inhibition activity arises from the polysulfated polymer present in the MoS reaction mixture, we used Sephadex G10 chromatography with 20% ethanol as eluent to separate the polymer from the monomers. The polymer, equivalent to peak 1 of Figure 1A, resolves readily from the monomeric entities peaks 2 and 3, and was obtained in ~10−14% isolated yield. When screened for HSV-1 viral infection inhibition activity, only peak 1 was found to be active, whereas peaks 2 and 3 were found to be inactive, thus indicating that a polydisperse, polysulfated molecule present in MoS reaction mixture was the origin of HSV-1 infection inhibition activity.

The anti-HSV-1 Sulfated Polymer Is a Sulfated Derivative of a Polymer Present in Raw Material, Morin. Two possibilities exist for the presence of polymeric substance in MoS reaction mixture. It is possible that (i) the active polymer is synthesized from the monomeric starting material morin during the sulfation reaction, or (ii) it is a product of sulfation of a polymeric substance already present in the raw material. Analysis of natural product morin by RP-HPLC using acetonitrile−water (8:2 v/v) mobile phase on a C-18 column showed a dominant peak at 16.5 min corresponding to starting material morin (Figure 2). However, the RP-HPLC profile showed additional small peaks between 9 and 15 min, which can merge in background noise, likely arising from small amounts of a polydisperse polymer. RP-HPLC screening of several independent sources of natural product morin (see "Experimental Section") showed nearly identical chromatograms, suggesting that this substance was consistently present.

The polymeric substance was isolated by exploiting its differential solubility in organic solvents. Whereas morin was found to possess good solubility in ethyl acetate or acetone, the extraneous polymer was nearly insoluble. The RP-HPLC profile of the ethyl acetate insoluble fraction showed multiple unresolved peaks between 9 and 17 min (Figure 2), which corresponded well with those found in crude morin. The peak shape indicates a highly polydisperse, heterogeneous polymer. Quantitative analysis of the ethyl acetate precipitation

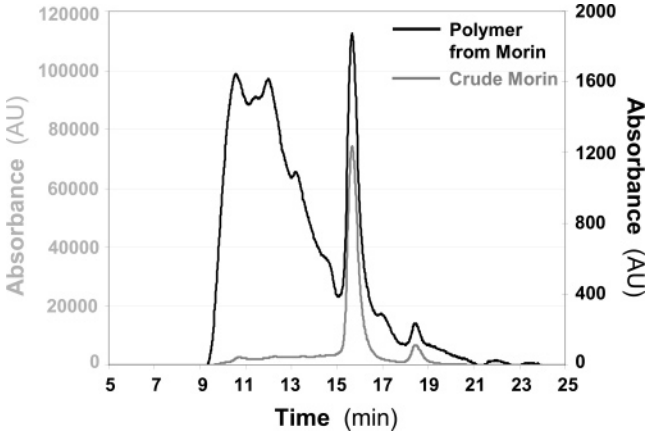

Figure 2. Reverse-phase HPLC analysis of morin (shown as gray profile and absorbance scale) and ethyl acetate insoluble substance (polymeric impurity of morin) (shown as black profile and absorbance scale). RP-HPLC was performed on an analytical column using acetonitrile−water (7:3 v/v) mobile phase at a flow rate of 0.5 mL/min, and peaks were detected at 279 nm. The polymeric substance folds into baseline for morin (gray profile, note the absorbance scale), which when enriched reveals a highly complex HPLC profile indicating a highly heterogeneous system. See text for details.

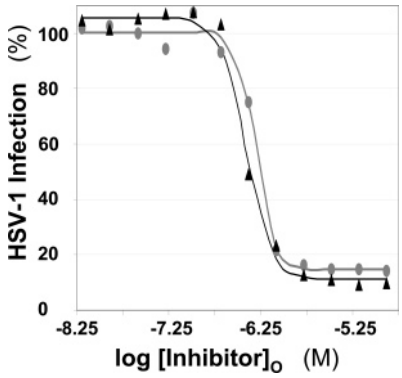

Figure 3. Inhibition of HSV-1 entry into cells by sulfated polymer obtained from morin sulfate reaction mixture (gray profile) and direct sulfation of ethyl acetate −insoluble substance (black profile). Inhibition assay involves the spectrophotometric determination of internalized viral particle in the presence and absence of inhibitors when exposed to a constant dose of the virus to HeLa cells at 37 °C. The spectrophotometric response in absence of inhibitor is assigned a value of 100% infection. The sigmoidal decrease in infection to increasing inhibitor concentration is fit to eq 1 to obtain the concentration of inhibitor necessary to achieve 50% inhibition (IC_{50}). See text for details.

step indicated that the polydisperse polymer was present in ~10% proportion from all three different sources of morin, an observation suggesting the likelihood of a biopolymeric nature.

To test whether the precipitated polymer is the origin of anti-HSV-1 activity, a sample of the polymer, free from monomeric morin, was prepared using centrifugal membrane filtration (see Experimental Section) and subjected to sulfation with triethylamine-sulfur trioxide complex (TEAST) in DMA at 65 °C. HSV-1 viral infection inhibition screening showed that this sulfated polymer was highly active (Figure 3). In fact, the inhibitory activity (IC_{50}) of 6.0 μg/mL found for this polymer was essentially identical to that of the sulfated polymer obtained through purification from reaction mixture (7.5 μg/mL). In contrast, the parent ethyl acetate-insoluble precipitate, the unsulfated polymer, was completely inactive. Finally, to ascertain that the sulfated polymer

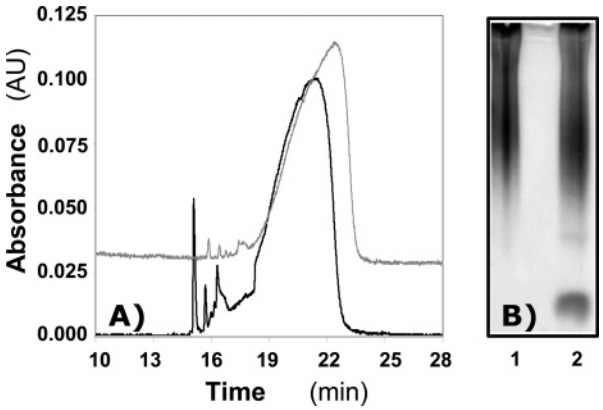

Figure 4. Equivalence of sulfated polymer obtained by isolation from morin sulfate reaction mixture (gray profile or lane 1) and direct sulfation of ethyl acetate/acetone insoluble substance (black profile or lane 2) using capillary electrophoretic profile (A) and polyacrylamide gel electrophoresis (B). Small differences in intensity of peaks observed between 15 and 17 min in the CE profile correspond to differences in proportion of monomeric morin sulfates. Likewise, the isolated band in lane 2 at the bottom of the profile, absent in lane 1, is due to monomeric morin sulfate. See text for details.

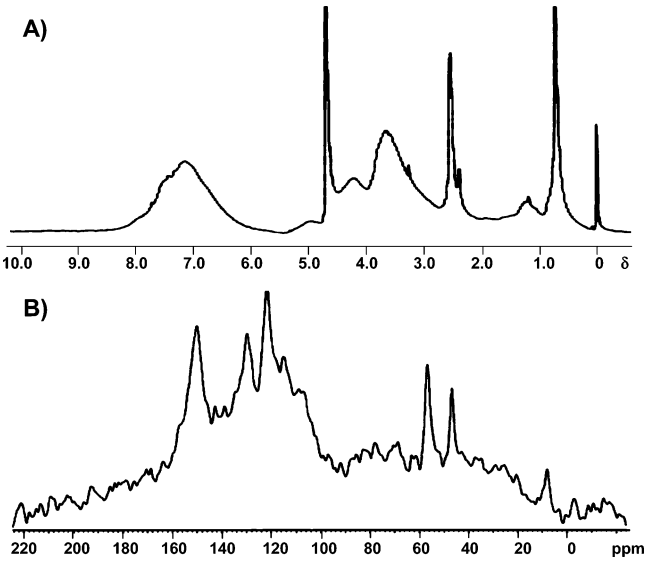

Figure 5. The 500 MHz ^{1}H (A) and 75 MHz ^{13}C (B) NMR spectrum of sulfated polymer. The ^{1}H NMR spectrum, obtained with a sample of M_R 1.9 kDa, shows extensive peak broadening for all peaks. The ^{13}C NMR spectrum was obtained with a 160 mg/mL sample of M_R 14.9 kDa at 60 °C acquired over 20 000 scans using a line broadening factor of 50 Hz. See text for details.

obtained from the ethyl acetate insoluble material was identical to the polymer purified from the MoS reaction mixture, comparative CE and PAGE techniques were used (Figure 4). Both the CE and the PAGE profiles of sulfated polymer obtained from sulfation of ethyl acetate or acetone precipitate, or chromatographic purification of MoS reaction mixture, were rather similar, suggesting that both of the sulfated polymers are identical.

The Unsulfated Polymer Is a Natural Product and not a Polymer of Morin. To confirm whether the polydisperse polymer is a product obtained on polymerization of morin during sulfation, we tested the ability of morin, freed of the polymeric substance, to polymerize. Sulfation was performed with triethylamine-sulfur trioxide complex, as for crude morin. Additionally, purified morin was heated with a catalytic amount boron trifluoride-diethyl ether complex or KOH in DMA at 60 °C to test whether mildly acidic or basic conditions initiate polymerization. Each reaction was continuously monitored on RP-HPLC using the protocol developed for separating morin and the polymer, yet no polymer formation could be detected in any of these reactions. These results indicate that morin is stable to acids and bases, and sulfation with TEAST complex does not give a polymeric species. This conclusion is also supported by literature data suggesting that polymers of flavones, which contain a 2-en-4-one moiety, are relatively unknown.[41] In contrast, polymers of flavans, which do not contain a 2-en-4-one structure, are abundant.[42,43] Further, the projected morin polymer, a flavonoid derivative, is expected to contain carbonyl groups, which were found to be absent in the isolated polymeric product (see below). Thus, the polymer isolated from morin sample is unlikely to have been formed synthetically from morin.

Spectroscopic Characterization of the Polymer. To assist in structure elucidation of both the unsulfated, native polymer and its sulfated counterpart, a sulfated polymeric fraction of M_R 1900 Da was isolated from the heterogeneous, polydisperse preparation using a combination of centrifugal filtration through molecular membrane (NMWC 5K) and preparative size-exclusion chromatography. The elemental analysis of parent unsulfated crude polymer, devoid of monomeric morin, revealed the presence of C, H, and O only, while its sulfated derivative contained C, H, O, S and Na elements, suggesting that the polymer does not contain N. The IR spectrum of the sulfated polymer shows a broad band in the region 3200−3600 cm^{-1} corresponding to −OH stretch and bands at 1610, 1500, 840, and 760 cm^{-1} (not shown) showing the presence of an aromatic structure, but more importantly displaying absence of certain groups, such as the carbonyl and triple bond.

The UV spectrum of the parent, unsulfated polymer in ethanol showed absorbance at 280 and 330 (sh) nm, indicating the presence of aromatic structure. The band at 280 nm underwent bathochromic shift of 26 nm in 1 N NaOH, which is characteristic of an acidic ionizable group such as a phenolic hydroxyl or carboxylic acid. Sulfation of the polymer resulted in hypsochromic shift of 12 nm in the band at 280. This change in λ_{MAX} to lower wavelengths by 6−10 nm is indicative of *O*-sulfation reaction.[29,30] Finally, addition of alkali to the sulfated polymer solution results in this band at 268 nm red shifting by 12 nm, indicating that the sulfated polymer retains some underivatized phenolic groups.

The ^{1}H NMR of 1.9 kDa sulfated polymer fraction in $^{2}H_2O$ at 25 °C showed several broad signals corresponding to significant polydispersity and heterogeneity in the sample (Figure 5A). The spectrum indicates the presence of aromatic protons between 6 and 8 δ, methine protons attached to multiple electron-withdrawing groups (OC*H*−Ph) at 5 δ, aromatic methoxys (ArOC*H*) at 4.2 δ, aliphatic methoxys (ROC*H*) at 3.6 δ, benzylic methylenes (ArCH) at 2.4 δ, and aliphatic methyls (RCH_3) and methylenes (RCH_2) at 0.9 and 1.2 δ. These broad resonances sharpen at higher temperatures, possibly because of enhanced flexibility, but do not resolve into sharp peaks for a more definite interpretation.

The signal at 0.9 δ suggests the presence of methyl groups in a rather hydrophobic environment of an anionic polymer. The observation that broad resonances dominate the ^{1}H NMR spectrum of a sulfated polymer with a relatively low M_R of 1900 Da (even at elevated temperature) suggests the presence of a highly networked polymer. More importantly, it indicates that the monomers making up the network are small (~100−200 Da).

The ^{13}C NMR spectrum of the sulfated polymer, recorded with a sample (80 mg/mL) at 60 °C and a line broadening factor of 50 Hz, showed broad peaks at 10 and 56 ppm corresponding to $-CH_3/CH_2$ and $-OCH_3$ groups, respectively, in addition to peaks for aromatic carbons in the range 115−160 ppm (Figure 5B). A broad signal at 48 ppm is also observed. This peak is unusual with very few organic groups resonating at this position and has been assigned to the HO*C*H− group, which typically resonate at ~50 ppm considering that the three-dimensional structure of the molecule may introduce special shielding environments that cause this 1−5 ppm shift (see below). This spectrum correlates well with the ^{1}H NMR spectrum discussed above. Also, the ^{13}C NMR spectrum shows absence of resonances in the region 180−200 ppm that correspond to carbonyl carbons, further supporting the FT-IR data.

The Polymer Is a Lignin Derivative. The biophysical properties of the polymeric natural product indicate that the polymer is polyphenol-based. Natural polyphenolic polymers include condensed tannins and lignins. Whereas condensed tannins, or proanthocyanidins,[42,43] are polymers of either flavan-3-ol, or flavan-4-ol, or flavan-3,4-diol monomers, lignins are polymers of phenylpropanoid monomers.[44−46] Both polymers demonstrate structural heterogeneity and complexity, yet condensed tannins are typically smaller with repeat units in the range of 2−8.

Two chemical tests, the acid-butanol[36] and the phloroglucinol[37] tests, characteristic for condensed tannins are available. The acid-butanol test relies on the acidic cleavage of polymeric tannin to flavanols, which are tested for their ability to complex with a ferric reagent. Complexation results in the development of a distinctive pink color, which can be quantified. In contrast, the phloroglucinol test relies on the ability to trap electrophilic intermediates formed during the acidic cleavage of the polymer with nucleophilic phloroglucinol. Both the acid-butanol and the phloroglucinol tests failed for the parent unsulfated polymer, indicating the absence of condensed tannin-type structure.

The above results suggest that our parent, unsulfated polydisperse polymer was not tannin, but most probably a lignin. Several lines of evidence support this conclusion. Lignin is a plant cell-wall material,[46] which is also a common source for commercial morin. In contrast, proanthocyanidins are typically isolated from grapes and wines.[45] Second, the observation that a fraction with M_R as low as 1900 Da shows broad ^{1}H NMR resonances suggests a highly networked polymer arising from small monomeric units with numerous different types of intermonomer linkages. The phenylpropanoid units of lignins typically include *p*-coumaryl, coniferyl, or sinapyl alcohols, which are small phenolic monomers (Figure 6). Varying self- and intermonomer

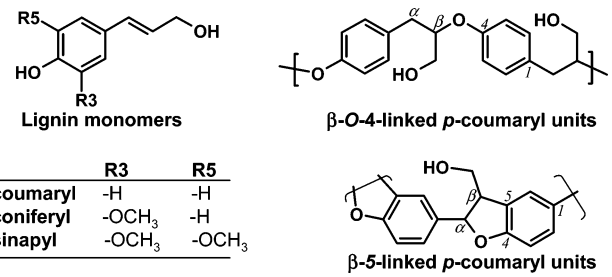

	R3	R5
***p*-coumaryl**	-H	-H
***p*-coniferyl**	-OCH_3	-H
***p*-sinapyl**	-OCH_3	-OCH_3

Figure 6. Structure of *p*-coumaryl, coniferyl, and sinapyl monomers, and two common inter-monomer linkages found in lignin polymer. The free −OH groups can be sulfated; thus *p*-coumaryl unit in β-*O*-4-linked and β-5 linked *p*-coumaryl polymer may contain a maximum of one sulfate per monomeric unit. Positions are either numbered (1,4,5) or labeled (α,β).

combinations of these small C6−C3 units result in a highly complex three-dimensional network-type structure. The spectroscopic data, discussed above, obtained on our polydisperse polymer, both sulfated and unsulfated, are consistent with a lignin structure. Finally, the ^{13}C and ^{1}H NMR spectra of purified low molecular weight lignosulfonate obtained from pine wood chip were essentially equivalent[47] (not shown) to that determined for our polymer (see Figure 5).

Mass Spectrometric Analysis of Lignin. Mass spectrometry forms an important tool in structural elucidation of lignins, although the heterogeneity and complexity of polymers represents a formidable challenge to overcome.[48,49] Further, attempts to identify higher oligomeric lignin fragment masses appear to fail because of instability of the polyphenolic structure.[49] Yet, MS remains the most sensitive technique to identify individual monomeric constituents and possibly identify the intermonomer linkages.

To identify the monomeric constituents present in our underivatized lignin, the polymer was partially depolymerized under acidic conditions. Resolution was achieved only with methanolic mobile phases under reverse-phase conditions, while ionization of the analytes appeared to work only in APCI negative mode. The reverse-phase chromatogram of depolymerized lignin indicated the presence of at least 15 major peaks in addition to numerous minor peaks and residual polymer hump (not shown). The negative ion APCI-MS spectra of all of the major peaks showed significant similarity of the mass peaks in the region 100−200 *m*/*z* suggesting a common backbone. The mass spectrum of a major peak eluting at the very end of the RP chromatogram displays a rich array of mass peaks in the region 100−300 *m*/*z* and several high MW peaks in the range 300−650 *m*/*z* (Figure 7). The mass pattern suggests the presence of more than one lignin oligomer. As shown in the figure, part of the mass spectrum, including major peaks at 283 and 265, can be interpreted as arising from oligomers of *p*-coumaryl alcohol with β-*O*-4 linkage (Figure 7). The interpretation is strengthened due to the observation of high molecular weight fragments (547, 542, and 529 *m*/*z*) that can be uniquely ascribed to a tetramer. However, this pattern does not rule out the possibility that condensed β-5 linkages are present, especially because the harsh depolymerization conditions employed can cause cleavage of several types of linkages.

Sulfation Level of Lignin Sulfate Fractions. To quantify the level of sulfation of lignin sulfate fractions, we deter-

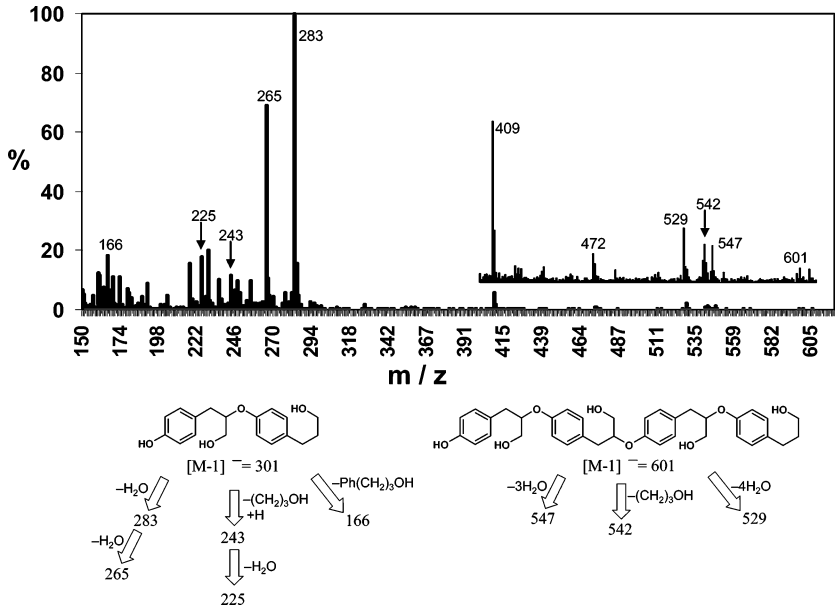

Figure 7. Mass spectral identification of lignin oligomers. Lignin sample was treated with 0.2 M HCl in dioxane−methanol and subjected to LC−MS analysis. The APCI-MS spectrum in the range 150−610 *m*/*z* of one of the peaks (out of nearly 15) is shown above. Inset shows the mass region 400−610 *m*/*z*, while structural analysis is depicted below. Although the overall spectrum is complex, many peaks can be identified uniquely as arising from a *β*-*O*-4 linked *p*-coumaryl alcohol monomers and its degradation products. See text for details.

mined the elemental composition of three lignin sulfate fractions, 39.4, 5.9, and 2.5 kDa. All three samples gave nearly identical proportions of C, H, O, and S elements, indicating essentially identical structural composition, except for differences in M_R. The average composition was found to be 33.6 ± 1.7%, 3.5 ± 0.2%, 41.3 ± 1.4%, and 11.7 ± 1.6% for C, H, O, and S, respectively. This observed composition is similar to a composition, 35.8% (C), 3.7% (H), 42.4% (O), and 10.6% (S), calculated for a linear *β*-5 polymer composed of *p*-coumaryl monomers containing one sulfate group and two H_2O. Likewise, an uncondensed linear *β*-*O*-4-linked lignin also satisfies the observed elemental composition, although less so than the condensed polymer. In contrast, the calculated value for S increases significantly if the sulfation level is assumed to be higher. It is important to note that, although the observed composition best matches the *p*-coumaryl containing lignin, coniferyl structures cannot be ruled out, especially because of the structural heterogeneity involved. These results suggest that the bioactive lignin sulfate sample is primarily made from *p*-coumaryl alcohol and contains one sulfate group per monomer.

Chromatographic and Electrophoretic Analysis of Lignin Sulfate. Lignin sulfate perhaps represents the first sulfated macromolecule that contains a three-dimensional network scaffold. This structure sharply contrasts the widely distributed sulfated polysaccharides, including heparin, heparan sulfate, and chondroitin sulfate, which are linear, unbranched polymers, or sulfated fucoidans, which are branched but not networked. The physicochemical properties of a three-dimensional network polymer are likely to be different from a linear polymer, and thus it was important to study its chromatographic and electrophoretic behavior.

The HP-SEC profile, performed on a column that resolves molecules less than 40 000 Da, displayed was a broad, fairly symmetrical, peak profile from ∼12 to ∼28 min, suggesting the presence of lignin chains with a wide range of molecular weights (1.5−40 kDa) and high polydispersity. This lignin sample was fractionated into four samples using sequential centrifugal membrane filtration with 100, 50, 10, and 5 kDa filters, while a fifth fraction corresponding to the smallest possible mixture of chains was isolated using Sephadex G25 gel (see Experimental Section). The HP-SEC profile of these five partially purified lignin sulfate fractions showed normally distributed peaks eluting at 17.2, 19.1, 21.0, 22.7, and 23.3 min (Figure 8A). The mobile phase contained 100 mM NaCl to minimize sample−matrix interaction, and the elution profile did not change significantly at higher concentrations of NaCl. Because SEC involves movement of molecules through the excluded volume, and does not involve penetration through gel pores, the elution times are expected to be independent of the shape of molecule, whether linear or three-dimensional network. Thus, assuming that the number of water molecules bound to lignin sulfate and the standards is the same, the M_R obtained through SEC is expected to more closely correspond to the true molecular weight. Using a standard curve obtained from the polysulfonate standards, the average molecular weights of lignin sulfate fractions were calculated to be 39.4, 14.9, 5.9, 2.5, and 1.9 kDa.

In contrast to the SEC chromatographic profile, the electrophoretic profile depends on the size and shape of the molecule in addition to its charge density. The PAGE profile of lignin sulfate and PSS was determined at several gel concentrations. As the concentration of the acrylamide monomer was increased from 6% to 12%, all PSS standards, except for PSS80, demonstrated a linear decrease in their electrophoretic mobility (log μ) (Figure 8B). For a macromolecule with size smaller than the pore size, this behavior follows the observations of Ferguson, extended by the Ogston−Morris−Rodbard−Chrambach model, in which retardation depends only on the radius of the migrating particle.[50,51] On a physical level, as the gel concentration increases, so do the number of cross-links resulting in

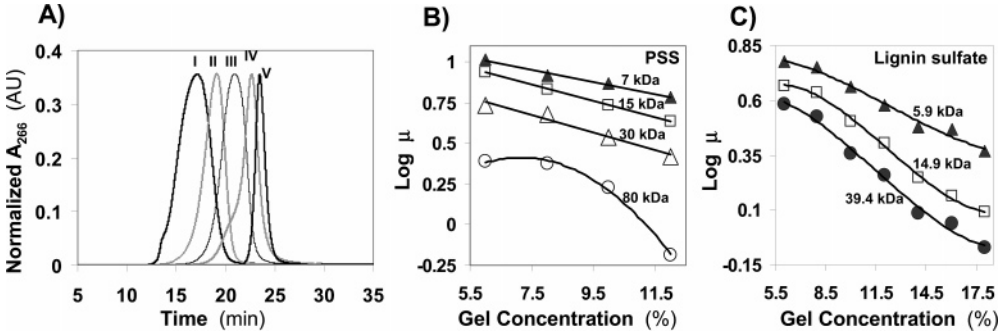

Figure 8. Chromatographic and electrophoretic analysis of lignin sulfate fractions. (A) HP-SEC of lignin sulfate fractions, (B) PAGE profile of PSS standards, and (C) PAGE profile of lignin sulfate fractions. Peaks were detected at 266 nm in HP-SEC, while samples were stained with high-iron diamine stain that detects sulfate groups. HP-SEC shows the profile for fractions I−V with M_R values of 39.4, 14.9, 5.9, 2.5, and 1.9 kDa, respectively. PAGE profiles for PSS standards 7, 15, 30, and 80 kDa (B) and for lignin sulfate fractions III, IV, and V (C). The solid line in the PAGE profile of each sample is a trendline and not a regressional fit. See text for details.

decrease in electrophoretic mobility. For a macromolecule, for example, PSS80, with size larger than the pore size, migration through pores may occur in a reptile-like movement wherein Ogston sieving is not possible, resulting in nonlinear Ferguson plots.

In contrast, the PAGE profile of lignin sulfate fractions exhibited unusual behavior. One, lignin sulfate fractions were retarded much greater than the corresponding PSS standards. For example, lignin sulfate fractions 39.4, 14.9, and 5.9 kDa display log μ values of 0.26, 0.40, and 0.58, respectively, in 12% gel in comparison to values of 0.42, 0.64, and 0.79 observed for PSS 30, 15, and 7 kDa standards (Figure 8C). Two, as the gel concentration decreases to 6%, the mobility of lignin sulfate fractions increases; however, the increase is not linear, in contrast to that observed for most PSS standards (Figure 8B). Whereas only PSS80 displays a nonlinear profile (Figure 8B), nonlinearity is evident in lignin sulfate samples with M_R values as low as 5.9 kDa. Both observations suggest that overall molecular shape of lignin sulfate is significantly different from linear polymers. Not unexpectedly, this originates from the network structure present in lignin sulfate. Yet, it is interesting to find that even small three-dimensionally networked lignin sulfate 5.9 kDa is retarded significantly more than PSS15. A major consequence of this phenomenon is that M_R determination of lignin sulfate using electrophoretic mobility is likely to be erroneous.

Discussion

Lignin, one of the most abundant biomaterial, was identified as a wood constituent more than 150 years ago. Yet, knowledge about lignin structure is still fragmentary. Lignins are highly heterogeneous, polydisperse polymers, which constitute the skeletal substance of all terrestrial plants. Their chemical structure depends on the botanical origin, the type of wood, the chemical composition of the biological fibers, the climatic conditions, the season of isolation, and the chemical processing during isolation.[44,46] Furthermore, it has been proposed that native lignin polymer is produced through random, nonenzymatic polymerization, which introduces another dimension of structural complexity.[52] Native lignin structure is rarely retained in the processed material as structural changes, for example, isomerization of double bonds, dehydration, and hydrogenation, may be introduced. Establishing lignin structure in detail is a challenging and arduous task.

The current work identifies presence of a lignin through an arduous chemical and biophysical structure elucidation process. While mass spectral analysis primarily suggests the presence of a β-*O*-4-linked *p*-coumaryl alcohol-based lignin, the presence of coniferyl alcohol cannot be excluded. In addition, considering the vigorous chemical degradation procedure used for LC−MS analysis, a β-5 linked polymer is also likely, a conclusion supported by elemental analysis. Several structural features remain to be elucidated as yet. For example, the ^{1}H and ^{13}C NMR spectra indicate the presence of hydrophobic methyls and methylenes, their location and number remain to be determined. The UV−vis study suggests the presence of underivatized phenolic groups, possibly at polymer termination points. Likewise, a number of high molecular weight peaks in the LC−MS spectra, possibly containing other intermonomeric linkages, remain unidentified. These native and non-native structures introduce significant structural complexity, yet the macromolecule that exhibits HSV-1 inhibitory activity is primarily a polymer containing an average of one sulfate group per monomer residue.

The electrophoretic property of lignin sulfate suggests an overall shape vastly different from linear sulfated polymers. The significant retardation in movement through acrylamide matrix, observed even for smaller lignin sulfates, suggests that these molecules cannot undergo reptile-like motion. This retardation is also aided by the presence of a large number of bound water molecules due to many surface sulfate groups. These sulfate bound water molecules on the surface of lignin sulfate can be thought of as equivalent to water molecules bound to polar and charged amino acid residues on protein surfaces. Thus, the overall molecular shape of lignin sulfate is expected to be globular, in contrast to sulfated polysaccharides that are known to be linear helices.[53]

The medicinal properties of lignins remain unknown. This report constitutes the first example of a lignin derivative, a sulfated form of lignin, as an inhibitor of HSV-1 entry into cells. The IC_{50} value of 6 μg/mL determined herein compares favorably with values of 0.5−10 μg/mL measured for heparin, heparan sulfate, dextran sulfate, fucan sulfate, and other sulfated polysaccharides.[14,16−22,24] Competitive inhibi-

tion of HSV-1 entry into cells is known to be highly dependent on the sulfation level of the competitor. Heparin, the most sulfated polysaccharide known, demonstrates the highest efficiency.[13,14] While a 15 kDa heparin chain would contain an average of nearly 88 negative charges, our lignin sulfate polymer, containing one sulfate group per monomer, would contain ~56. (The average charge density of heparin is ~3.5 negatively charged groups (OSO_3^- + COO^-) per disaccharide. Nearly 50 monomers (each 300 Da) are present in a heparin chain with M_R value of 15 kDa, thus giving ~88 negative charges. On the other hand, lignin sulfate with an M_R of 15 kDa would contain 56 monomers (each 268 Da) with an average of one negative charge per monomer.) These fewer sulfate groups in lignin may be closer to the number in heparan sulfate, which is known to be less sulfated than heparin.[9,10] Further, just as with heparan sulfate, our lignin sulfate structure may possess pockets of higher charge density originating from the differential reactivity of −OH groups in parent heterogeneous lignin. Thus, the co-incidental optimal sulfation level, coupled with significant structural heterogeneity, is likely the origin for the anti-HSV-1 activity of lignin sulfate.

Structurally, lignin sulfate represents a rich combination of substructures that represent many different options for interaction. The presence of multiple aromatic rings introduces hydrophobic forces, while unsulfated −OH groups make available hydrogen-bonding capability. Further, sulfation introduces the capability to form ionic interactions, while the bound water molecules, which can be released upon binding to a protein, introduce a favorable entropic factor. Thus, important enthalpic forces including hydrogen bonding, ionic, and hydrophobic, and entropic forces that govern nearly all interactions are present in lignin sulfate. Further, the structural possibilities afforded by many different types of linkages and different types of monomers suggest that lignin sulfate may possess structural richness thought to be present in heparan sulfate. Further work is needed to exploit this opportunity.

Acknowledgment. We thank Professor Sally Ralph (USDA-Agricultural Research Service, Department of Forestry, University of Wisconsin, Madison, WI) for her comments and generous gift of lignin samples. This work was supported by grants from the National Heart, Lung, and Blood Institute (RO1 HL 069975-U.R.D.), the American Heart Association (0256286U), the A. D. Williams Foundation, and the National Institute for Allergy and Infectious Diseases (RO1 AI 057860-D.S.).

References and Notes

(1) Corey, L.; Spear, P. G. Infections with herpes simplex viruses. *N. Engl. J. Med.* **1986**, *314*, 686−691.
(2) Corey, L.; Spear, P. G. Infections with herpes simplex viruses (2). *N. Engl. J. Med.* **1986**, *314*, 749−757.
(3) Spear, P. G. Herpes simplex virus: receptors and ligands for cell entry. *Cell. Microbiol.* **2004**, *6*, 401−410.
(4) Shukla, D.; Spear, P. G. Herpesviruses and heparan sulfate: an intimate relationship in aid of viral entry. *J. Clin. Invest.* **2001**, *108*, 503−510.
(5) Spear, P. G.; Eisenberg, R. J.; Cohen, G. H. Three classes of cell surface receptors for alphaherpesvirus entry. *Virology* **2000**, *275*, 1−8.
(6) Spear, P. G. Entry of alphaherpesviruses into cells. *Semin. Virol.* **1993**, *4*, 167−180.
(7) Shriver, Z.; Liu, D.; Sasisekharan, R. Emergining views of heparan sulfate glycosaminoglycan structure/activity relationships modulating dynamic biological functions. *Trends Cardiovasc. Med.* **2002**, *12*, 71−77.
(8) Bernfield, M.; Gotte, M.; Park, P. W.; Reizes, O.; Fitzgerald, M. L.; Lincecum, J.; Zako, M.; Functions of cell surface heparan sulfate proteoglycans. *Annu. Rev. Biochem.* **1999**, *68*, 729−777.
(9) Esko, J. D.; Lindahl, U. Molecular diversity of heparan sulfate. *J. Clin. Invest.* **2001**, *108*, 169−173.
(10) Rabenstein, D. L. Heparin and heparan sulfate: structure and function. *Nat. Prod. Rep.* **2002** *19*, 312−331.
(11) Shukla, D.; Liu, J.; Blaiklock, P.; Shworak, N. W.; Bai, X.; Esko, J. D.; Cohen, G. H.; Eisenberg, R. J.; Rosenberg, R. D.; Spear, P. G. A novel role for 3-O-sulfated heparan sulfate in herpes simplex virus 1 entry. *Cell* **1999**, *99*, 13−22.
(12) Tiwari, V.; Clement, C.; Duncan, M. B.; Chen, J.; Liu, J.; Shukla, D. A role for 3-O-sulfated heparan sulfate in cell fusion induced by herpes simplex virus type 1. *J. Gen. Virol.* **2004**, *85*, 805−809.
(13) Feyzi, E.; Trybala, E.; Bergstrom, T.; Lindahl, U.; Spillmann, D. Structural requirement of heparan sulfate for interaction with herpes simplex virus type 1 virions and isolated glycoprotein C. *J. Biol. Chem.* **1997**, *272*, 24850−24857.
(14) Herold, B. C.; Gerber, S. I.; Polonsky, T.; Belval, B. J.; Shaklee, P. N.; Holme, K. Identification of structural features of heparin required for inhibition of herpes simplex virus type 1 binding. *Virology* **1995**, *206*, 1108−1116.
(15) Lycke, E.; Johansson, M.; Svennerholm, B.; Lindahl, U. Binding of herpes simplex virus to cellular heparan sulphate, an initial step in the adsorption process. *J. Gen. Virol.* **1991**, *72*, 1131−1137.
(16) Herold, B. C.; Siston, A.; Bremer, J.; Kirkpatrick, R.; Wilbanks, G.; Fugedi, P.; Peto, C.; Cooper, M. Sulfated carbohydrate compounds prevent microbial adherence by sexually transmitted disease pathogens. *Antimicrob. Agents Chemother.* **1997**, *41*, 2776−2780.
(17) Dyer, A. P.; Banfield, B. W.; Martindale, D.; Spannier, D. M.; Tufaro, F. Dextran sulfate can act as an artificial receptor to mediate a type-specific herpes simplex virus infection via glycoprotein B. *J. Virol.* **1997**, *71*, 191−198.
(18) Preeprame, S.; Hayashi, K.; Lee, J. B.; Sankawa, U.; Hayashi, T. A novel antivirally active fucan sulfate derived from an edible brown alga, *Sargassum horneri*. *Chem. Pharm. Bull. (Tokyo)* **2001**, *49*, 484−485.
(19) Lee, J. B.; Hayashi, K.; Hashimoto, M.; Nakano, T.; Hayashi, T. Novel antiviral fucoidan from sporophyll of *Undaria pinnatifida* (Mekabu). *Chem. Pharm. Bull. (Tokyo)* **2004**, *52*, 1091−1094.
(20) Ponce, N. M.; Pujol, C. A.; Damonte, E. B.; Flores, M. L.; Stortz, C. A. Fucoidans from the brown seaweed *Adenocystis utricularis*: extraction methods, antiviral activity and structural studies. *Carbohydr. Res.* **2003**, *338*, 153−165.
(21) Hayashi, T.; Hayashi, K.; Maeda, M.; Kojima, I. Calcium spirulan, an inhibitor of enveloped virus replication, from a blue-green alga *Spirulina platensis*. *J. Nat. Prod.* **1996**, *59*, 83−87.
(22) Carlucci, M. J.; Pujol, C. A.; Ciancia, M.; Noseda, M. D.; Matulewicz, M. C.; Damonte, E. B.; Cerezo, A. S. Antiherpetic and anticoagulant properties of carrageenans from the red seaweed *Gigartina skottsbergii* and their cyclized derivatives: correlation between structure and biological activity. *Int. J. Biol. Macromol.* **1997**, *20*, 97−105.
(23) Zacharopoulos, V. R.; Phillips, D. M. Vaginal formulations of carrageenan protect mice from herpes simplex virus infection. *Clin. Diagn. Lab. Immunol.* **1997**, *4*, 465−468.
(24) Witvrouw, M.; De Clercq, E. Sulfated polysaccharides extracted from sea algae as potential antiviral drugs. *Gen. Pharmacol.* **1997**, *29*, 497−511.
(25) Mazumder, S.; Ghosal, P. K.; Pujol, C. A.; Carlucci, M. J.; Damonte, E. B.; Ray, B. Isolation, chemical investigation and antiviral activity of polysaccharides from *Gracilaria corticata* (Gracilariaceae, Rhodophyta). *Int. J. Biol. Macromol.* **2002**, *31*, 87−95.
(26) Hasui, M.; Matsuda, M.; Okutani, K.; Shigeta, S. In vitro antiviral activities of sulfated polysaccharides from a marine microalga (*Cochlodinium polykrikoides*) against human immunodeficiency virus and other enveloped viruses. *Int. J. Biol. Macromol.* **1995**, *17*, 293−297.
(27) Nyberg, K.; Ekblad, M.; Bergstrom, T.; Freeman, C.; Parish, C. R.; Ferro, V.; Trybala, E. The low molecular weight heparan sulfate-mimetic, PI-88, inhibits cell-to-cell spread of herpes simplex virus. *Antiviral Res.* **2004**, *63*, 15−24.

(28) Vaheri, A.; Ikkala, E.; Saxen, E.; Penttinen, K. Biological actions of polyanions. A comparative study of the effect of herpes virus, blood coagulation, red blood cells and growth behavior of cells on a glass surface. *Acta Pathol. Microbiol. Scand.* **1964**, *62*, 340−348.

(29) Gunnarsson, G. T.; Desai, U. R. Interaction of sulfated flavanoids with antithrombin: Lessons on the design of organic activators. *J. Med. Chem.* **2002**, *45*, 4460−4470.

(30) Gunnarsson, G. T.; Desai, U. R. Designing small, nonsugar activators of antithrombin using hydropathic interaction analyses. *J. Med. Chem.* **2002**, *45*, 1233−1243.

(31) Gunnarsson, G. T.; Desai, U. R. Exploring new nonsugar sulfated molecules as activators of antithrombin. *Bioorg. Med. Chem. Lett.* **2003**, *13*, 579−583.

(32) Gunnarsson, G. T.; Riaz, M.; Adams, J.; Desai, U. R. Synthesis of per-sulfated flavonoids using 2,2,2-trichloro ethyl protecting group and their factor Xa inhibition potential. *Bioorg. Med. Chem.* **2005**, *13*, 1783−1789.

(33) Montgomery, R. I.; Warner, M. S.; Lum, B. J.; Spear, P. G. Herpes simplex virus − 1 entry into cells mediated by a novel member of the TNF/NGF receptor family. *Cell* **1996**, *87*, 427−436.

(34) Warner, M. S.; Geraghty, R. J.; Martinez, W. M.; Montgomery, R. I.; Whitbeck, J. C.; Xu, R.; Eisenberg, R. J.; Cohen, G. H.; Spear, P. G. A cell surface protein with herpesvirus entry activity (HveB) confers susceptibility to infection by mutants of herpes simplex virus type 1, herpes simplex virus type 2, and pseudorabies virus. *Virology* **1998**, *246*, 179−189.

(35) Munakata, H.; Isemura, M.; Yosizawa, Z. An application of the high-iron diamine staining for detection of sulfated glycoproteins (glycopeptides) in electrophoresis on cellulose acetate membrane. *Tohoku J. Exp. Med.* **1985**, *145*, 251−257.

(36) Porter, L. J.; Hrstich, L. N.; Chan, B. G. The conversion of procyanidins and prodelphinidins to cyanidin and delphinidin. *Phytochemistry* **1986**, *25*, 223−230.

(37) Kennedy, J. A.; Jones, G. P. Analysis of proanthocyanidins cleavage products following acid-catalysis in the presence of excess phloroglucinol. *J. Agric. Food Chem.* **2001**, *49*, 1740−1746.

(38) Dantuluri, M.; Desai, U. R. Capillary electrophoresis of sulfated molecules. *Recent Res. Dev. Anal. Biochem.* **2003**, *3*, 169−186.

(39) Duchemin, V.; Le Potier, I.; Troubat, C.; Ferrier, D.; Taverna, M. Analysis of intact heparin by capillary electrophoresis using short end injection configuration. *Biomed. Chromatogr.* **2002**, *16*, 127−133.

(40) Linhardt, R. J.; Pervin, A. Separation of negatively charged carbohydrates by capillary electrophoresis. *J. Chromatogr., A* **1996**, *720*, 323−335.

(41) Geiger, H. In *The Flavonoids. Advances in Research Since 1986*; Harborne, J. B., Ed.; Chapman and Hall: London, 1994.

(42) Ferreira, D.; Li, X.-C. Oligomeric proanthocyanidins: naturally occurring O-heterocycles. *Nat. Prod. Rep.* **2000**, *17*, 193−212.

(43) Ferreira, D.; Slade, D. Oligomeric proanthocyanidins: naturally occurring O-heterocycles. *Nat. Prod. Rep.* **2002**, *19*, 517−541.

(44) Glasser, W. G. Lignin. In *Pulp and Paper − Chemistry and Chemical Technology*, 3rd ed.; Casey, J. P., Ed.; Wiley and Sons: New York, 1980; pp 39−111.

(45) Singleton, V. L. Tannins and the qualities of wines. In *Plant Polyphenols*; Hemingway, R. W., Laks, P. E., Eds.; Plenum Press: New York, 1992.

(46) Sarkanen, K. V.; Ludwig, C. H. *Lignins: Occurrence, Formation, Structure and Reactions*; Wiley-Interscience: New York, 1971.

(47) Ralph, S. A. USDA-Agricultural Research Service, Department of Forestry, University of Wisconsin, Madison, WI. Personal Communication.

(48) Reale, S.; Di Tullio, A.; Spreti, N.; De Angelis, F. Mass spectrometry in the biosynthetic and structural investigation of lignins. *Mass Spectrom. Rev.* **2004**, *23*, 87−126.

(49) Banoub, J. H.; Delmas, M. Structural elucidation of the wheat straw lignin polymer by atmospheric pressure chemical ionization tandem mass spectrometry and matrix-assisted laser desorption/ionization time-of-flight mass spectrometry. *J. Mass Spectrom.* **2003**, *38*, 900−903.

(50) Ferguson, K. A. Starch-gel electrophoresis − Application to the classification of pituitary proteins and polypeptides. *Metabolism* **1964**, *13*, 985−1002.

(51) Rodbard, D.; Chrambach, A. Unified theory for gel electrophoresis. *Proc. Natl. Acad. Sci. U.S.A.* **1970**, *65*, 970−977.

(52) Freudenberg, K.; Neish, A. C. *Constitution and Biosynthesis of Lignin*; Springer-Verlag: New York, 1968; p 132.

(53) Capila, I.; Linhardt, R. J. Heparin-protein interactions. *Angew. Chem., Int. Ed.* **2002**, *41*, 390−412.

BM0503064